

# A target tracking method based on adaptive occlusion judgment and model updating strategy

Zhiming Cai<sup>Corresp., Equal first author, 1, 2</sup>, Zhuangzhuang Wang<sup>Equal first author, 1</sup>, Jianchao Huang<sup>1</sup>, Shujing Chen<sup>1</sup>, Huabin He<sup>1</sup>

<sup>1</sup> School of Electronic, Electrical Engineering and Physics, Fujian University of Technology, Fuzhou, Fujian, China

<sup>2</sup> National Demonstration Center for Experimental Electronic Information and Electrical Technology Education, Fujian University of Technology, Fuzhou, Fujian, China

Corresponding Author: Zhiming Cai  
Email address: caizm@fjut.edu.cn

Target tracking is an important research in the field of computer vision. Despite the rapid development of technology, there still remains difficulties in balancing the overall performance for target occlusion, motion blur, etc. To address the above issue, we propose an improved kernel correlation filter tracking algorithm with adaptive occlusion judgement and model updating strategy (called Aojmus) to achieve robust target tracking. Firstly, the algorithm fuses color-naming (CN) and histogram of gradients (HOG) features as a feature extraction scheme and introduces a scale filter to estimate the target scale, which reduces tracking error caused by the variations of target features and scales. Secondly, the Aojmus introduces four evaluation indicators and a double thresholding mechanism to determine whether the target is occluded and the degree of occlusion respectively. The four evaluation results are weighted and fused to a final value. Finally, the updating strategy of the model is adaptively adjusted based on the weighted fusion value and the result of the scale estimation. Experimental evaluations on the OTB-2015 dataset are conducted to compare the performance of the Aojmus algorithm with four other comparable algorithms in terms of tracking precision, success rate, and speed. The experimental results show that the proposed Aojmus algorithm outperforms all the algorithms compared in terms of tracking precision. The Aojmus also exhibits excellent performance on attributes such as target occlusion and motion blur in terms of success rate. In addition, the processing speed reaches 74.85 fps, which also demonstrates good real-time performance.

# A target tracking method based on adaptive occlusion judgment and model updating strategy

Zhiming Cai<sup>1,2✉\*</sup>, Zhuangzhuang Wang<sup>1\*</sup>, Jianchao Huang<sup>1</sup>, Shujing Chen<sup>1</sup>, and Huabin He<sup>1</sup>

<sup>1</sup>School of Electronic, Electrical Engineering and Physics, Fujian University of Technology, Fuzhou, China

<sup>2</sup>National Demonstration Center for Experimental Electronic Information and Electrical Technology Education, Fujian University of Technology, Fuzhou, China

Corresponding author:

Zhiming Cai\*

Email address: caizm@fjut.edu.cn

## ABSTRACT

Target tracking is an important research in the field of computer vision. Despite the rapid development of technology, there still remains difficulties in balancing the overall performance for target occlusion, motion blur, etc. To address the above issue, we propose an improved kernel correlation filter tracking algorithm with adaptive occlusion judgement and model updating strategy (called Aojmus) to achieve robust target tracking. Firstly, the algorithm fuses color-naming (CN) and histogram of gradients (HOG) features as a feature extraction scheme and introduces a scale filter to estimate the target scale, which reduces tracking error caused by the variations of target features and scales. Secondly, the Aojmus introduces four evaluation indicators and a double thresholding mechanism to determine whether the target is occluded and the degree of occlusion respectively. The four evaluation results are weighted and fused to a final value. Finally, the updating strategy of the model is adaptively adjusted based on the weighted fusion value and the result of the scale estimation. Experimental evaluations on the OTB-2015 dataset are conducted to compare the performance of the Aojmus algorithm with four other comparable algorithms in terms of tracking precision, success rate, and speed. The experimental results show that the proposed Aojmus algorithm outperforms all the algorithms compared in terms of tracking precision. The Aojmus also exhibits excellent performance on attributes such as target occlusion and motion blur in terms of success rate. In addition, the processing speed reaches 74.85 fps, which also demonstrates good real-time performance.

## INTRODUCTION

Motion target tracking (Lu and Xu, 2019; Wang et al., 2021) is one of the most active research areas in computer vision. With the continuous improvement of hardware facilities and the rapid development of artificial intelligence technology, motion target tracking technology is widely used in intelligent video surveillance (Zeng et al., 2020), human-computer interaction (Zhou and Liu, 2021), medical diagnosis (Al-Battal et al., 2021) and other fields. In the field of intelligent video surveillance, target tracking technology is commonly used in monitoring of vehicle violations and has been proved to be effective. In the field of medical diagnosis, tracking technology is frequently used in tracking microscopic items like cells. In terms of human-computer interaction, tracking technology is mostly utilized in robot vision and virtual environments, which primarily use visual technology to provide the tracking effect similar to human eyes. In the past two decades, target tracking technology has made tremendous developments. However, tracking targets are often limited by complex application environments, such as different illumination changes, interference from complex backgrounds, changes in their own scales, and occlusion by other objects. Therefore, improving the precision and robustness of tracking algorithms in complex environments and satisfying real-time applications become important research topics in visual target tracking.

46 Nowadays, the mainstream algorithms of target tracking can be classified into two categories. One is  
47 based on correlation filtering (Wei and Kang, 2017; Meng and Li, 2019), which determines the correlation  
48 region by establishing a correlation filter to find the maximum response value in the two adjacent frames,  
49 and then lock the target. Compared with the earlier tracking algorithms based on optical flow method (Xiao  
50 et al., 2016) and feature matching (Uzkent et al., 2015), the advantages for this category are fast speed and  
51 good robustness in the case of target occlusion, illumination change and motion blur (Liu et al., 2017).  
52 Another is based on deep learning (Li et al., 2016), which uses convolutional neural networks training to  
53 extract object features in the last frame and matches the object in the next frame. That is, the object is  
54 continually tracked during training. For one thing, the former is inferior to the latter when dealing with  
55 complex scenarios, such as target occlusion, out-of-view, scale variation etc. For another, the latter tracks  
56 object more slowly. Therefore, finding a solution not only meets the demands of accurate tracking in a  
57 variety of complex scenarios, but also achieves fast running are still an active research area. In this work,  
58 a target tracking algorithm based on adaptive occlusion judgment and model updating strategy, called  
59 Aojmus, is proposed to address the poor tracking performance in complex scenarios mentioned above.  
60 The Aojmus is designed on the basis of KCF algorithm and integrated with correlation filtering method  
61 which has the advantage in processing speed.

62 The contributions of this work can be summarized in three folds:

- 63 1. We propose to fuse CN and HOG features as the feature representation of the tracked target, which  
64 improves the discrimination and re-detection ability. Meanwhile, the scale filter is introduced to  
65 solve the defect of poor tracking precision of the target due to scale change.
- 66 2. We design four kinds of occlusion judgment indicators to solve tracking failure which caused by  
67 occlusion. These four indicators can adaptively judge the occlusion of the target during tracking. A  
68 double threshold mechanism is introduced to judge the degree of occlusion, which determines the  
69 update strategy of the tracker.
- 70 3. We use a weighted fusion strategy to fuse the results of occlusion judgments to ensure that the  
71 model update rate of the tracker changes dynamically with the judgment results of each frame,  
72 avoiding the tracking drift problem caused by fixed model update rate of most trackers.

73 The rest of this article is organized as follows. In "Literature Review", related works about target  
74 tracking are surveyed. In "Preliminaries", some prerequisites of the methodology are introduced. In  
75 "Methodology", we describe the architecture of the proposed algorithm, including statistical analysis,  
76 algorithm design and related parameter setting. In "Experiments and analysis", we compare and analyze  
77 the performance of the algorithm in quantitative and qualitative aspects. In "Conclusion", we summarize  
78 this study and discuss possible future work.

## 79 LITERATURE REVIEW

80 Bolme et al. (Bolme et al., 2010) were the first to apply the correlation filtering method to target tracking  
81 and proposed the MOSSE algorithm, which achieves tracking speed of 669 fps, but with a slightly poor  
82 precision of 43.1%. To solve the problem of insufficient samples of MOSSE algorithm, Henriques et  
83 al. (Henriques et al., 2012) proposed CSK algorithm, which acquired a large number of samples through  
84 the method of cyclic shift. Moreover, the computational complexity is reduced by frequency domain  
85 processing, and thereby a robust and accurate filter is obtained. Subsequently, Henriques et al. proposed  
86 the Kernelized Correlation Filter(KCF) (Henriques et al., 2015) tracking algorithm on the basis of CSK,  
87 which utilized HOG (Histogram of Oriented Gradients) feature instead of grayscale feature and introduced  
88 a circular matrix to reduce the computational effort. The algorithm also incorporates multi-channel data to  
89 improve the operation speed and meet the requirement of real-time in the process of tracking. Inspired by  
90 the scale pooling technique, Li et al. (Yang and Zhu, 2014) and Danelljan et al. (Danelljan et al., 2014a)  
91 proposed SAMF and DSST algorithms respectively, which solved the problem of scale adaptation of KCF  
92 algorithm. The SAMF algorithm fused HOG feature and CN (Danelljan et al., 2014b)(Color-Naming)  
93 feature for the first time on the basis of KCF, which improved the tracking precision, but the speed  
94 is significantly reduced. Similarly, the DSST algorithm also achieved scale adaption, but the overall  
95 performance is inferior. Danelljan et al. (Danelljan et al., 2017a) used convolutional neural network (CNN)  
96 to extract depth features on the feature model of the target while keeping the motion model (cyclic matrix)

97 and observation model (correlation filter) unchanged, achieving a significant increase in precision and  
 98 success rate. The research interest in correlation filtering-based target tracking has declined because the  
 99 precision is difficult to improve further when dealing with target occlusion, disappearance, or non-rigid  
 100 object tracking. In recent years, some representative studies have still emerged, such as ASRCF (Dai  
 101 et al., 2019), ARCF (Huang et al., 2019), and PRCF (Sun et al., 2019).

102 Another class of target tracking algorithms is based on deep learning (Li et al., 2016), which uses  
 103 convolutional neural networks for feature extraction and classification of targets to achieve target tracking.  
 104 Some of them incorporate correlation filtering and deep learning, such as the HCF (Ma et al., 2015). The  
 105 MDNet algorithm proposed by Nam et al. (Nam and Han, 2016) was one of the early algorithms that used  
 106 deep learning alone to implement target tracking. The algorithm trains each domain separately while  
 107 updating the parameters of the shared layer during training so that these parameters can be adapted to all  
 108 datasets. When tracking, MDNet uses a pre-trained CNN network to track the target and thereby locate  
 109 the target. Here are some similar algorithms, such as SiamDW (Zhang and Peng, 2019), SiamCAR (Guo  
 110 et al., 2020) and HiFT (Cao et al., 2021), etc. Despite the superior performance of deep learning-based  
 111 tracking algorithms in achieving tracking precision, they still face the disadvantages of insufficient initial  
 112 training samples and slow tracking speed.

## 113 PRELIMINARIES

114 In this section, to help establish an understanding of the essential elements involved in the proposed  
 115 methodology, the Kernelized Correlation Filter (KCF), classifier training, fast detection and model  
 116 updating are illustrated in advance.

### 117 Kernelized correlation filter

118 The core idea of the kernel correlation filtering (KCF) algorithm is to calculate the matching degree  
 119 between the predicted region and the target by establishing a kernel function based on the ridge regression.  
 120 By moving the complex calculation to the frequency domain with fast Fourier transform, the fast tracking  
 121 for target is achieved. Similar to most discriminative tracking algorithms, KCF algorithm also performs  
 122 target detection before filter model training. It firstly trains a model of the initial position of the target,  
 123 then detects whether the target exists in the prediction region of the next frame, and finally uses Gaussian  
 124 kernel to calculate the correlation between two adjacent frames and determines the position of the target  
 125 according to its maximum response value in the target region. The basic principles of the kernel correlation  
 126 filtering algorithm, including classifier training, fast detection and model update, are described below.

### 127 Classifier training

The classifier  $f(x) = \langle w, \varphi(x) \rangle$  is obtained by training ridge regression. Let  $(x_i, y_i)$  be the training sample,  
 where  $y_i$  is the regression expectation corresponding to sample  $x_i$ . The ridge regression on the training  
 sample yields the linear regression function  $f(x) = w^T x_i$ . To prevent the overfitting phenomenon, the  
 classifier needs to be regularized as follows:

$$\min_w \sum_{i=1}^N (f(x_i) - y_i)^2 + \lambda \|w\|^2 \quad (1)$$

where  $w$  is the classifier parameter and  $\lambda$  is the regularization parameter. The closed-form solution of the  
 above equation is:

$$w = (X^T X + \lambda I)^{-1} X^T y \quad (2)$$

In the process of generating a large amount of information of target and background using the circular  
 matrix, the feature space formed by the sample set appears nonlinear. Therefore, Gaussian kernel function  
 $\varphi(x_i)$  is introduced for linear transformation, and get  $f(x) = w^T x_i = w^T \varphi(x_i)$ , where  $w = \sum_{i=1}^N \alpha_i x_i$ . So  
 far, the solution of  $w$  is transformed to the solution of coefficient  $\alpha$ , which eventually yields:

$$\alpha = (K + \lambda I)^{-1} y \quad (3)$$

where  $K$  is the kernel correlation matrix. To reduce the complexity of the calculation, Equation (3) is  
 transformed into the frequency domain with the discrete Fourier transform(DFT). Then the solution

becomes:

$$\hat{\alpha} = \frac{\hat{y}}{k^{xx} + \lambda} \quad (4)$$

128 The purpose of classifier training is to solve the weight coefficient  $\alpha$ , where  $k^{xx}$  is the first row element of  
129 the kernel cycle matrix  $K$ , and  $\hat{\cdot}$  denotes the DFT of vector.

### 130 Fast detection and model updating

After classifier training, in order to locate the target position of the current frame, the KCF algorithm uses the target position of the previous frame as a template, then detects it in the candidate region  $z$  of the current frame and determines the target position by finding the maximum value of  $f(z) = \alpha^T \varphi(X) \varphi(z)$ . To increase the calculation speed, the KCF algorithm transfers the solution from the time domain to the frequency domain as follows:

$$\hat{f}(z) = \hat{k}^{xz} \odot \hat{\alpha} \quad (5)$$

131 where  $k^{xz}$  denotes the kernel correlation between the target sample  $x$  and the candidate detection region  
132  $z$ ,  $\hat{f}(z)$  represents the response distribution in the candidate region and the position where its maximum  
133 value is located indicates the actual position of the target in the current frame.

To ensure each frame in the video sequence can be processed, the KCF algorithm uses linear interpolation to update the filter template  $\hat{\alpha}_t$  and the target feature template  $\hat{x}_t$  as follows:

$$\begin{cases} \hat{\alpha}_t = (1 - \eta) \hat{\alpha}_{t-1} + \eta \hat{\alpha} \\ \hat{x}_t = (1 - \eta) \hat{x}_{t-1} + \eta \hat{x} \end{cases} \quad (6)$$

134 where  $\eta$  denotes the model update rate and  $t$  is time stamp.

## 135 METHODOLOGY

136 As target occlusion, scale variation, illumination variation affect the performance of tracking, it is of great  
137 significance to conquer such problems. The KCF algorithm increases the training samples through the  
138 circular matrix, which in turn improves the tracking accuracy. Meanwhile, by transferring to the frequency  
139 domain to avoid matrix inversion operations, the computation is greatly reduced.

140 However, the KCF algorithm often fails to track in the case of target occlusion or target loss because  
141 the update model learns the features of the occluded object and causes the model to get the wrong target  
142 features in the accumulation of subsequent frames, which in turn leads to tracking failure. In addition, the  
143 tracking box of KCF algorithm cannot meet the scale variation of the target, which can also greatly reduce  
144 the precision of tracking. To address these problems, this paper proposes a target tracking algorithm,  
145 call Aojmus, based on an adaptive occlusion judgment and model update strategy. The flow chart of the  
146 algorithm is shown in Fig. 1.

147 In this section, we describe the specific implementation of Aojmus, including feature fusion, scale  
148 estimation, occlusion judgment and model updating.

### 149 Feature fusion design

150 The HOG features can effectively depict the local contour and shape information of the target and are  
151 very robust to illumination changes, but are poorly adapted to target deformation and fast motion. The CN  
152 features can well represent the global color information of the target and have excellent stability to target  
153 deformation and fast motion, but are sensitive to illumination and color changes. Therefore, we employ  
154 linear fusion of HOG feature and CN feature (Xie and Zhao, 2021) to achieve feature complementarity  
155 and improve tracking precision.

The process of linear weighted fusion of these two feature vectors is as follows:

$$v_{hc} = \delta v_{hog} + (1 - \delta) v_{cn} \quad (7)$$

156 where  $v_{hog}$ ,  $v_{cn}$ ,  $v_{hc}$  represent HOG feature, CN feature and fused feature respectively, and  $\delta$  is the  
157 weighted coefficient of feature fusion. In this paper, set  $\delta = 0.5$  to ensure that the advantages of HOG  
158 and CN feature can be fully utilized.

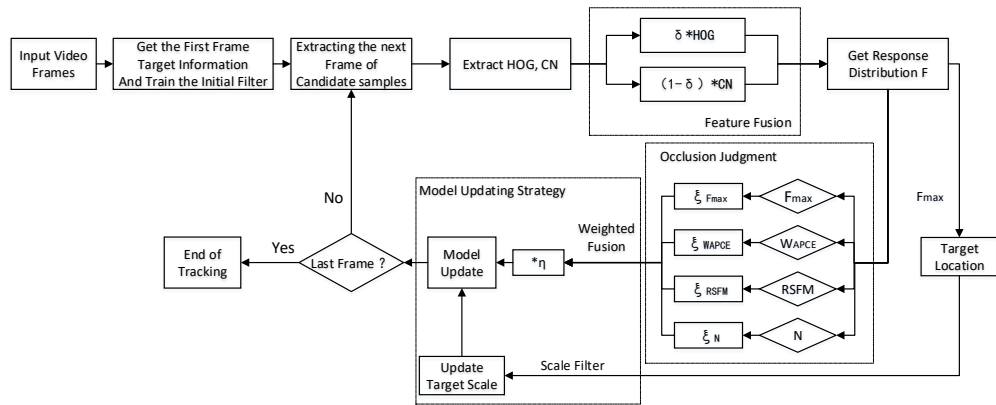


Figure 1. Flow chart of Aojmus algorithm.

### 159 Multi-scale estimation

160 The scale variation of target is one of the important factors affecting the tracking results. As the position  
 161 change of two consecutive frames is often larger than the scale change, like DSST (Danelljan et al.,  
 162 2014a), this paper first uses a two-dimensional position filter to determine the position information and  
 163 then implements scale evaluation by training a one-dimensional scale filter.

Let  $f$  be the training sample and  $h$  be the optimal correlation filter. The minimum cost function is solved with ridge regression as follows:

$$\varepsilon = \left\| \sum_{l=1}^d h^l \odot f^l - g \right\|^2 + \lambda \sum_{l=1}^d \|h^l\|^2 \quad (8)$$

where  $l \in \{1, \dots, d\}$  is the feature dimension,  $g$  represents the regression expectation corresponding to the training sample  $f$ , and  $\lambda$  is the regularization factor. The scaling filter can be obtained by solving the above equation in Fourier domain:

$$H^l = \frac{\bar{G}F^l}{\sum_{k=1}^d \bar{F}^k F^k + \lambda} = \frac{A_l^l}{B_l} \quad (9)$$

where  $\bar{G}$  represents complex conjugate of the DFTs of correlation outputs and  $\lambda$  is introduced to avoid zero denominator in case of the zero frequency component in  $f$ . By detecting the image block  $z$  in the new frame, we can obtain the response of scale filter as:

$$y = F^{-1} \left\{ \frac{\sum_{l=1}^d \bar{A}_l^l Z^l}{B + \lambda} \right\} \quad (10)$$

Up to this point, the response value of the scale filter can be calculated from Equation (10), and a new scale estimate can be determined based on the result of the maximum value. The selection principle of target sample size for scale evaluation is as follows:

$$a^n P \times a^n R, n \in \left\{ \left\lfloor \frac{-(s-1)}{2} \right\rfloor, \dots, \left\lfloor \frac{(s-1)}{2} \right\rfloor \right\} \quad (11)$$

164 where  $P$  and  $R$  are respectively the width and height of the target in the previous frame,  $a = 1.02$  is the  
 165 scale factor,  $s = 33$  is the length of the scale filter.

### 166 Adaptive occlusion judgment and model updating strategy

167 Target occlusion often occurs during tracking. In this section, we make a detailed analysis and propose an  
 168 adaptive judgment method. Using the original model update rate in the KCF algorithm, the response of  
 169 occlusion is analyzed with the FaceOcc1 image sequence in the OTB2015 (Wu et al., 2015) dataset as an  
 170 example.

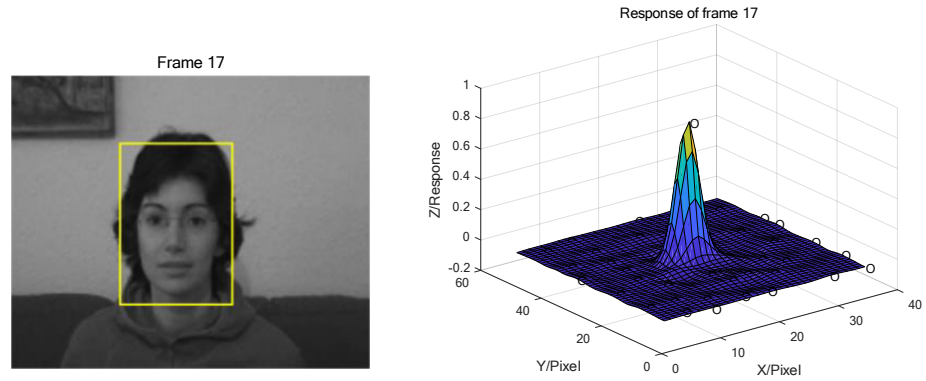


**Figure 2.** Tracking results and response distribution at frame 17 of the FaceOcc1 sequence without occlusion. Photo credit: Visual Tracker Benchmark.

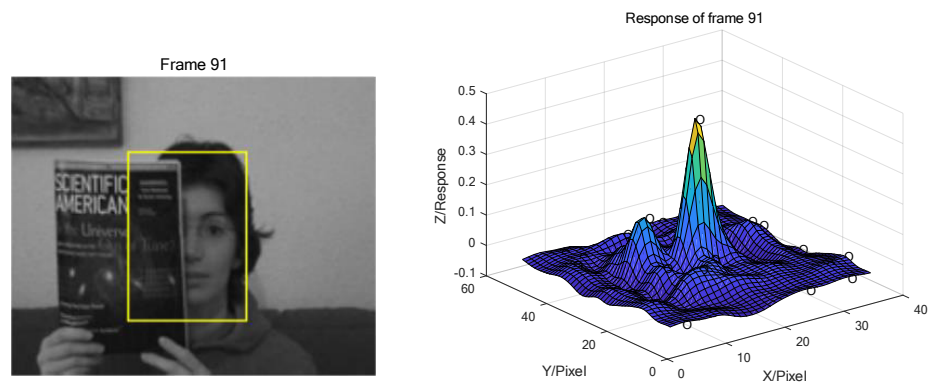


**Figure 3.** Tracking results and response distribution when occlusion appears at frame 91 of FaceOcc1 sequence. Photo credit: Visual Tracker Benchmark.

171 From the response distribution in Fig. 2, it can be seen that the main peak of the response in target  
 172 box during tracking without occlusion is dominated and there is no other obvious peaks. The maximum  
 173 peak response is close to 1. When the occlusion exists, as shown in Fig. 3, the maximum peak response  
 174 decreases significantly, and the rest of the peak responses increase and become more prominent. It can  
 175 be concluded that when the occlusion occurs, the fixed model update strategy learns the features of the  
 176 occlusion and applies this feature to the search of the next frame which leading to the appearance of other  
 177 peaks besides the main peak. Hence, the presence of occlusion can be determined based on the response  
 178 distribution of the target.

Let  $F_{max}$  be the maximum peak response in each frame. The number of peak response points that exceed the maximum peak response by a certain proportion, denoted as  $N$ , can be expressed as:

$$N = \sum \left( (F'_{max} > \zeta F_{max}) \in S \right) \quad (12)$$

179 where  $F'_{max}$  denotes the peak response other than the maximum peak,  $S$  represents the target area, and  $\zeta$  is  
 180 a proportionality coefficient which is set to 0.1 in this paper.

181 Besides the two judgment indicators of  $F_{max}$  and  $N$ , two more judgment indicators,  $APCE$  (Average  
 182 Peak-to-Correlation Energy, (Wang et al., 2017)) and  $RSFM$  (Ratio between the Second and First Major  
 183 mode, (Lukežić et al., 2017)) are introduced in this paper to ensure the robustness of the occlusion  
 184 judgment.

The  $APCE$  can well reflect the variation of response and changes significantly when the target is obscured. It can be expressed as follows:

$$W_{APCE} = \frac{|F_{max} - F_{min}|^2}{\text{mean} \left( \sum_{w,h} (F_{w,h} - F_{min})^2 \right)} \quad (13)$$

185 where  $F_{min}$  denotes the minimum value of the response, and  $F_{w,h}$  denotes the response value of pixel in  
 186  $w$ -th row and  $h$ -th column. When occlusion appears, the value of  $W_{APCE}$  will decrease significantly.

The  $RSFM$  reflects the prominence of the main peak in the response map and is defined as follows:

$$RSFM = 1 - \min \left( \frac{F_{second}}{F_{max}}, \frac{1}{2} \right) \quad (14)$$

187 where  $F_{second}$  represents the response value of the second peak. The larger the value of  $RSFM$  is, the more  
 188 prominent the main peak will be and the higher reliability the tracking will have, and vice versa.

189 In this paper, we use the four evaluation indicators mentioned above,  $F_{max}$ ,  $N$ ,  $W_{APCE}$  and  $RSFM$ , to  
 190 determine whether the target is occluded or not. To verify the four indicators, we select the first 200  
 191 frames of the video sequence in FaceOcc1 for test. The relevant results of these four indicators for each  
 192 frame are calculated and their cumulative averages are shown in Fig. 4.

193 As shown in Fig. 4, the evaluation indicators fluctuate significantly between frame 85 to 100. The  
 194  $F_{max}$ ,  $W_{APCE}$ ,  $RSFM$  are relatively low whereas  $N$  is relatively high, which indicates the existence of  
 195 severe occlusion. By comparing the moments when occlusion appears in the original video sequence,  
 196 it can be found that the above four indicators satisfy well for the judgment of occlusion as they are  
 197 complementary to some extent.

In order to accurately determine whether occlusion exists and the degree of occlusion, this paper implements adaptive evaluation by setting dynamic double thresholds. The thresholds are selected based on the average value of each evaluation indicator for the previous  $t - 1$  frames, namely:

$$\theta(R)_n = \frac{\kappa_n}{t-1} \sum_{i=2}^t R^i, R \in (F_{max}, W_{APCE}, RSFM, N), n = 1, 2 \quad (15)$$

198 where,  $\kappa$  denotes the weighted coefficient, and  $\theta(R)$  denotes the threshold of the corresponding evaluation  
 199 indicator. For every indicator, there are two thresholds. The weighted coefficient  $\kappa$  of each evaluation  
 200 indicator is obtained by analyzing the Cumulative Average curve in Fig. 4, as shown in Table 1.

201 As can be seen from Equation (14), the value of  $F_{second}$  rises sharply when there is severe occlusion  
 202 in current frame, resulting the output of  $RSFM$  to be 0.5. When it occurs, the lower limit of  $\theta(RSFM)_2$

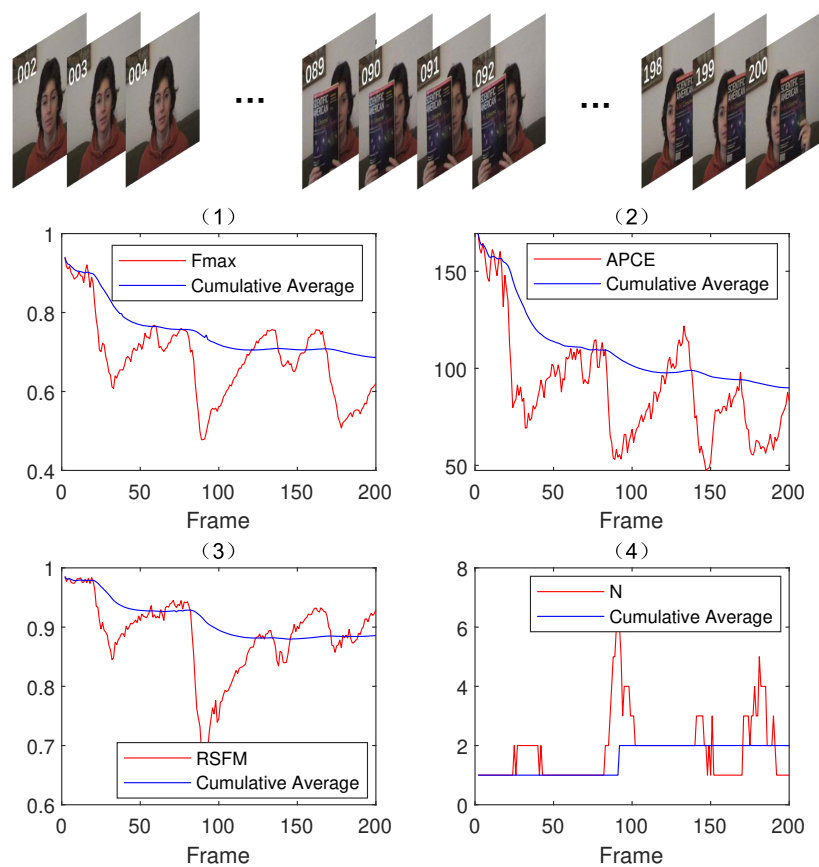


**Figure 4.** Line graphs of  $F_{max}$ ,  $W_{APCE}$ ,  $RSFM$  and  $N$  for the front 200 frames of FaceOcc1 as an example. Photo credit: Visual Tracker Benchmark.

**Table 1.** Weighted coefficients of double thresholds for each evaluation indicator.

	$\kappa_1$	$\kappa_2$
$\theta(F_{max})_n$	1	0.85
$\theta(W_{APCE})_n$	1	0.7
$\theta(RSFM)_n$	1	
$\theta(N)_n$	1	

**Table 2.** Output values of the four judgment indicators  $\mu_n$ .

	$\mu_1$	$\mu_2$	$\mu_3$
$\xi_{F_{max}}$	1	1.2	1.5
$\xi_{W_{APCE}}$	1	0.8	0.5
$\xi_{RSFM}$	1	1.2	1.5
$\xi_N$	1.2		1

203 in Table 1 is set to 0.5 particularly. And as  $N$  is usually not sensitive to occlusion, it is set to a single  
204 threshold for simplicity.

When occlusion appears, the fixed model update rate  $\eta$  will cause the tracker to learn the information of the occlusion object and lead to tracking drift. In this paper, the Aojmus algorithm adaptively generates a suitable model update rate according to the degree of occlusion in current frame. When occlusion occurs, the model update rate is appropriately increased to ensure that the target information of the part not occluded in the tracking frame is fully learned by the model so as to enhance the model's recognition capability, which can be used for accurate localization in next frame. The update strategy is defined as:

$$\xi_R = \begin{cases} \mu_1 & R \geq \theta(R)_1 \\ \mu_2 & \theta(R)_1 > R > \theta(R)_2 \\ \mu_3 & else \end{cases} \quad (16)$$

205 where,  $R \in (F_{max}, W_{APCE}, RSFM, N)$ ,  $\mu_n (n = 1, 2, 3)$  represent the output values of occlusion judgment.  
206 They are concluded from experiments, as shown in Table 2.

There are four judgment results in the improved algorithm. In order to guarantee that  $\xi_R$  can accurately reflect the degree of occlusion, this paper uses a weighted fusion of the four output  $\xi_R$  to obtain the final model update rate as follows:

$$\xi = \frac{\xi_{F_{max}}^2 + \xi_{W_{APCE}}^2 + \xi_{RSFM}^2 + \xi_N^2}{sum(\xi_R)} \quad (17)$$

207 Finally, we substitute the final model update rate into Equation (6) to obtain:

$$\begin{cases} \hat{\alpha}_t = (1 - \xi * \eta) \hat{\alpha}_{t-1} + \xi * \eta \hat{\alpha} \\ \hat{x}_t = (1 - \xi * \eta) \hat{x}_{t-1} + \xi * \eta \hat{x} \end{cases} \quad (18)$$

208 The proposed algorithm, Aojmus, is presented in Algorithm 1 .

## 209 EXPERIMENTS AND ANALYSIS

210 In this section the proposed Aojmus algorithm is compared with the other 4 relatively excellent tracking  
211 algorithms. We use three metrics to evaluate the performance of the algorithm, and select the representative  
212 video sequences to compare and analyze the tracking effect.

### 213 Experimental environment and parameters

214 The platform for the experiments in this paper is Matlab 2018a, and the hardware environment is a  
215 computer with Intel(R) Xeon(R) CPU E5-2620 v3 @ 2.40GHz and 16GB RAM. The parameters of the  
216 algorithm are set as follows: the regularization parameter  $\lambda = 10^{-4}$  and the initial model update rate  
217  $\eta = 0.02$ .

218 In this paper, 66 video sequences provided by OTB-2015 are used for experimental verification.  
219 The dataset contains 11 attributes of common scenarios in target tracking, such as occlusion (OCC),  
220 deformation (DEF), illumination variation (IV), motion blur (MB), out-of-plane rotation (OPR), fast  
221 motion (FM), out-of-view (OV), in-plane rotation (IPR), low resolution (LR), scale variation (SV), and  
222 background clutter (BC). The performance evaluations are carried out with quantitative and qualitative  
223 analysis.

**Algorithm 1** : Aojmus**Input:**

Current frame  $I_t$ ; The video for tracking  $S_{videos}$ ;  
 Target position  $p_{t-1}$  and scale  $s_{t-1}$  of previous frame;  
 The target feature template,  $\hat{x}_{t-1}$  and the filter template,  $\hat{\alpha}_{t-1}$ ;  
 The scale model  $A_{t-1}^{scale}, B_{t-1}^{scale}$ .

**Output:**

Target position  $p_t$  and scale  $s_t$  of current frame;  
 The updated target feature template,  $\hat{x}_t$  and filter template,  $\hat{\alpha}_t$ ;  
 The updated scale model  $A_t^{scale}, B_t^{scale}$ .

- 1: **for** each  $I_t \in S_{videos}$  **do**
- 2:     Sample the new patch  $z^t$  from  $I_t$  at  $p_{t-1}$ ;
- 3:     Extract a scale sample  $z_{scale}$  from  $I_t$  at  $p_t$  and  $s_{t-1}$ ;
- 4:     Extract the HOG and CN features and fused with Equation (7);
- 5:     Calculate the response  $\hat{f}(z^t)$  with Equation (5), and get  $F_{max}$ ;
- 6:     Calculate  $N$ ,  $W_{APCE}$  and  $RSFM$  with Equation (12), (13) and (14), and adaptively judge whether there is occlusion and the scope;
- 7:     Get the  $\xi_R$  and  $\xi$  by Equation (16) and (17);
- 8:     Compute the scale correlations  $y_{scale}$  using  $z_{scale}$ ,  $A_{t-1}^{scale}$  and  $B_{t-1}^{scale}$  in Equation (10);
- 9:     Set  $s_t$  to the maximum of  $y_{scale}$ ;
- 10:     Use Equation (18) to update  $\hat{x}_t$  and  $\hat{\alpha}_t$  with  $\hat{x}_{t-1}$  and  $\hat{\alpha}_{t-1}$  adaptively;
- 11:     Use Equation (9) to update  $A_t^{scale}$  and  $B_t^{scale}$  with  $A_{t-1}^{scale}$  and  $B_{t-1}^{scale}$ .
- 12:     Return  $p_t$  and the updated  $\hat{x}_t$ ,  $\hat{\alpha}_t$ ,  $A_t^{scale}$ ,  $B_t^{scale}$ .
- 13: **end for**

224 **Experimental comparison and analysis**225 **Quantitative analysis**

In order to evaluate the performance of the algorithm in this paper, MSCF (Zheng et al., 2021), Staple (Bertinetto et al., 2016), fDSST (Danelljan et al., 2017b) and KCF algorithms with high performance were selected for comparison. Three statistical criteria of precision (Wu et al., 2013)(shorted as  $Pr$ ), success rate (Wu et al., 2013)(shorted as  $Sr$ ) and tracking speed (shorted as  $Ts$ ) were used for evaluation respectively. The  $Pr$  refers to the error of center position, namely the Euclidean distance in pixel unit,  $D_t$ , between the center of tracking box for each frame and the actual center in the benchmark. The final result is expressed with the average of errors.

$$Pr = \frac{D_t}{n} \quad (19)$$

226     The smaller the value of  $Pr$  is, the closer the tracked target center to the actual location is and the  
 227     better the algorithm performs in terms of precision.

Let  $O_t$  be the overlap between the tracking box in the current frame,  $B_t$ , and the actual box in benchmark,  $B_{bt}$ . It can be expressed as:

$$O_t = \frac{area(B_t \cap B_{bt})}{area(B_t \cup B_{bt})} \quad (20)$$

The success rate,  $Sr$ , is expressed as the average of  $O_t$  whose value is greater than the given threshold in the whole video sequence.

$$Sr = \frac{1}{n} \sum_{t=1}^n O_t \quad (21)$$

228     The value of  $Sr$  reflect the number of frames whose tracking box is closer to the real rectangle box.  
 229     Obviously, the greater the  $Sr$  is, the better the performance of the algorithm will be.

The tracking speed,  $Ts$ , refers to the number of video frames processed by the algorithm in each second, also known as frame rate with the unit of FPS (frames per second). It is defined as follows :

$$Ts = \frac{F_{total}}{t_{total}} \quad (22)$$

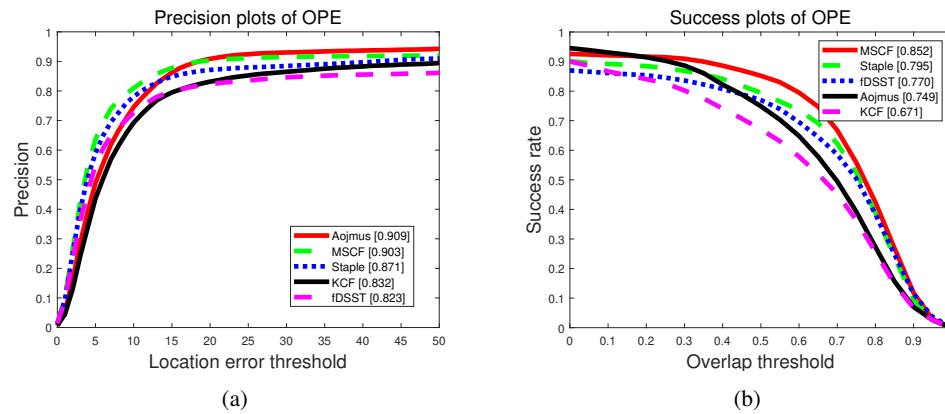


**Figure 5.** The tracking precision plots (a) and success rate plots (b) of our algorithm and others on OTB-2015.

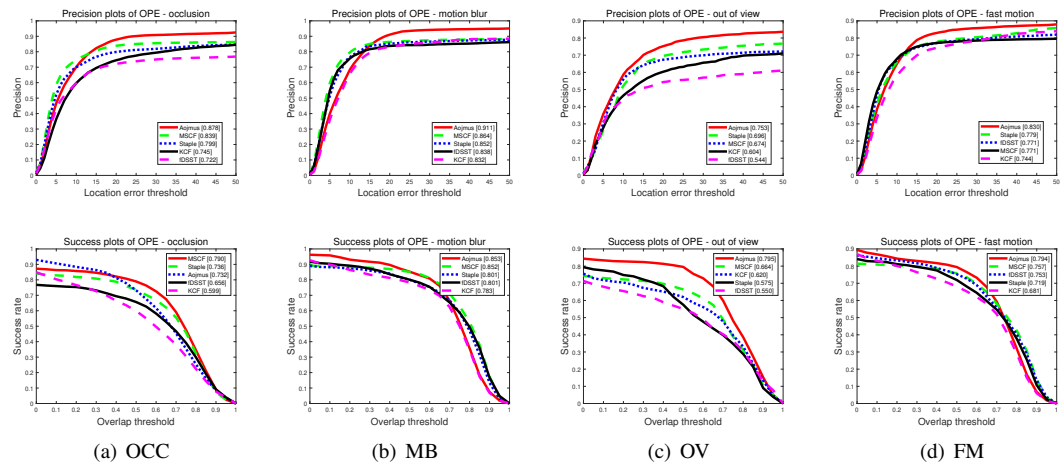


**Figure 6.** Precision plots (above) and success rate plots (below) under OCC (a), MB (b), OV (c), FM (d)

230 where,  $F_{total}$  indicates the total number of frames of the video sequence, and  $t_{total}$  is the time taken by the  
 231 algorithm to run the whole video sequence.

232 To evaluate the performance of the proposed algorithm, Aojmus, we make a comparison with other  
 233 four algorithms, MSCF, Staple, fDSST and KCF on OTB-2015 as shown in Fig. 5-Fig. 6 and Table 3  
 234 -Table 5. The evaluation method is OPE (One-Pass Evaluation), which means that after initializing the  
 235 target, the whole video sequence is run at once. The location error threshold for precision plots and the  
 236 overlap threshold for success rate plots are set as 20 pixels and 0.5, respectively.

237 Fig. 5 illustrates the precision and success rate of these five algorithms for running the whole sequences  
 238 at once on the OTB-2015 dataset, from which the precision and success rate of Aojmus can be obtained  
 239 are 0.909 and 0.749, respectively. Compared with others, the Aojmus performs the best in terms of  
 240 precision and has improved 0.5% than the second ranked MSCF algorithm. Though the success rate is not  
 241 outstanding, the Aojmus still shows high performance for OCC, MB, OV, and FM as shown in Fig. 6.

242 Table 3 and Table 4 respectively show the precision and success rate of the five algorithms under 11  
 243 attributes. As it can be seen that the Aojmus algorithm performs best on 10 of these attributes. In terms of  
 244 success rate, the Aojmus appears more robust in dealing with fast motion, motion blur and out of view  
 245 problems. Despite the disadvantages in other aspects, the Aojmus is not much inferior to other excellent  
 246 algorithms. For the tracking speed, though the Aojmus is inferior to fDSST and KCF as shown in Table 5,  
 247 it outperforms others in other aspects as shown in Fig. 5 and Fig. 6. From the above comparisons, the  
 248 Aojmus exhibits good overall performance.

**Table 3.** Comparison of precision on different attributes.

Algorithms	OCC	DEF	FM	IPR	MB	OV	OPR	SV	IV	BC	LR
Aojmus	<b>0.878</b>	0.900	<b>0.830</b>	<b>0.916</b>	<b>0.911</b>	<b>0.753</b>	<b>0.895</b>	<b>0.992</b>	<b>0.906</b>	<b>0.892</b>	<b>0.996</b>
MSCF	0.839	<b>0.941</b>	0.771	0.878	0.864	0.674	0.881	0.868	0.876	0.877	0.988
Staple	0.799	0.878	0.779	0.860	0.852	0.696	0.816	0.851	0.863	0.860	0.797
fDSST	0.722	0.777	0.771	0.799	0.838	0.544	0.759	0.796	0.876	0.891	0.731
KCF	0.722	0.813	0.744	0.818	0.832	0.604	0.803	0.805	0.863	0.882	0.785

**Table 4.** Comparison of success rate on different attributes.

Algorithms	OCC	DEF	FM	IPR	MB	OV	OPR	SV	IV	BC	LR
Aojmus	0.732	0.727	<b>0.794</b>	0.762	<b>0.853</b>	<b>0.795</b>	0.718	0.651	0.684	0.744	0.662
MSCF	<b>0.790</b>	<b>0.891</b>	0.757	<b>0.805</b>	0.852	0.664	<b>0.799</b>	<b>0.794</b>	<b>0.851</b>	<b>0.863</b>	<b>0.931</b>
Staple	0.736	0.798	0.719	0.765	0.801	0.575	0.724	0.726	0.793	0.787	0.604
fDSST	0.656	0.710	0.753	0.733	0.801	0.550	0.678	0.715	0.815	0.827	0.705
KCF	0.599	0.661	0.681	0.662	0.783	0.620	0.628	0.520	0.644	0.750	0.285

**Table 5.** Comparison of tracking speed of our algorithm and others.

Algorithms	Frames Per Second (FPS)
Aojmus	74.85
MSCF	16.01
Staple	9.28
fDSST	83.29
KCF	219.03

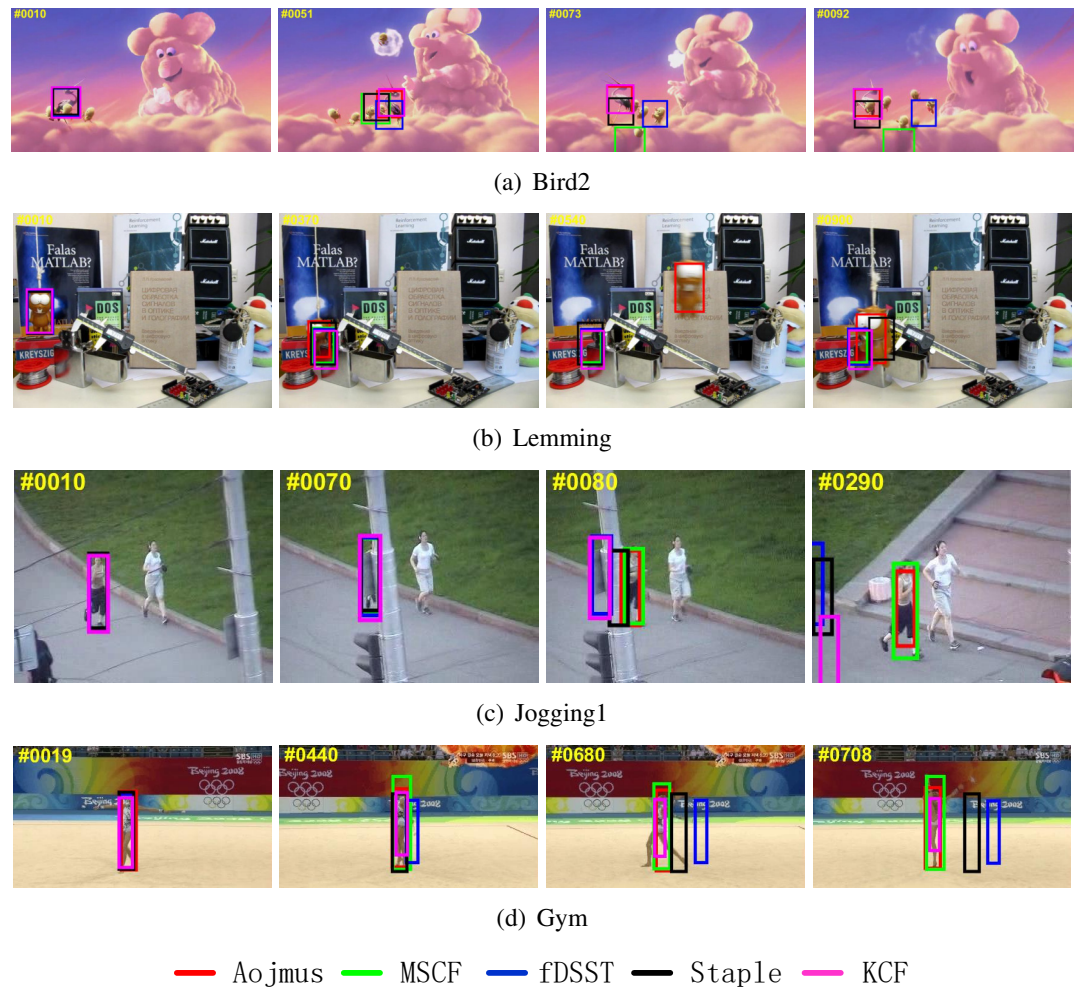


**Figure 7.** Tracking results of different algorithms on Bird2, Lemming, Jogging1 and Gym. Photo credit: Visual Tracker Benchmark.

#### 249 **Qualitative analysis**

250 Like our previous work in (Wang et al., 2022), in order to better verify the advantages of the proposed  
 251 algorithm, four groups of representative video sequences are selected for analysis, as shown in Fig. 7.

252 The video sequence of Bird2 contains OCC, DEF, FM, IPR, and OPR attributes. In frame 10, all  
 253 the five tracking algorithms work properly. With the progress of tracking, the MSCF, fDSST, and KCF  
 254 algorithms begin to show significant tracking drift at frame 51 affected by occlusion, deformation, and  
 255 rotation problems. From frame 73, only the Aojmus and Staple can track accurately after the target(bird)  
 256 flips.

257 The video sequence of Lemming contains IV, SV, OCC, FM, OPR, and OV attributes. From frame 10  
 258 to frame 370, as the target is not significantly affected by occlusion, fast motion and illumination changes,  
 259 and the position of the target does not change after the occlusion, all the algorithms can track the target  
 260 accurately. After the 370th frame, the occluded target reappears. As the tracking models of the other  
 261 algorithms use fixed update rate and learn non-target information, they are unable to locate the target  
 262 again in the subsequent frames, while the Aojmus can maintain accurate localization until the end of  
 263 tracking. In addition, comparing the tracking boxes at 900th frame, it can be shown the Aojmus is also  
 264 well adaptive to the scale change of the target.

265 The video sequence of Jogging1 contains OCC, DEF, and OPR attributes. The target is heavily  
 266 occluded at frames 70 to 80. When the target reappears, the Aojmus is able to accurately locate the target  
 267 using adaptive occlusion judgment and continue the model update to ensure that tracking is performed

268 reliably. The other algorithms except MSCF fail to cope with the occlusion problem.

269 The video sequence of Gym contains SV, DEF, IPR, and OPR attributes. At frame 19, the target  
270 begins to rotate and deform, and all algorithms can basically guarantee normal tracking. When it comes to  
271 440th frame, the fDSST algorithm shows obvious drift, and fails to track the target. With the increase of  
272 target deformation and rotation, only the Aojmus, MSCF and KCF can keep tracking properly till frame  
273 680. The Aojmus can adjust the tracking box with the scale of target dynamically whereas the MSCF and  
274 KCF fail to do so.

275 The above experimental results show that the Aojmus proposed in this paper can cope well with a  
276 variety of influence appearing in the tracking process, especially in the aspects of occlusion, scale change  
277 and deformation. On the whole, the Aojmus is robust for target tracking in complex scenes, and typically  
278 provides a new idea to deal with occlusion problems.

## 279 CONCLUSIONS

280 In target tracking, scholars have conducted in-depth research in many aspects to be able to predict the  
281 position of moving targets more accurately. However, due to the variability of the tracked target and  
282 scene, it is not easy to develop an algorithm that takes into account the above 11 influencing factors  
283 simultaneously, especially in solving the problems of target occlusion, deformation and scale variation.  
284 The previous researches, which typically uses one judgment indicator to address the occlusion problem,  
285 can't obtain outstanding overall performance. In this study, considering the complex scenarios and the  
286 requirement of mutual-complementarity of technologies, we propose four indicators,  $F_{max}$ ,  $N$ ,  $W_{APCE}$   
287 and  $RSFM$  as conditions to make the occlusion judgment more accurate. Moreover, we introduce an  
288 adaptive model updating strategy, fuse the results of the occlusion judgement and apply them into the  
289 model updating, which improves the precision in predicting the target position. As tracking is processed  
290 frame by frame where different influence factors may be encountered, this study presents a dynamic  
291 dual thresholds to compose the update strategy and achieves an accurate judgment of the existence and  
292 degree of occlusion, which solves the problem of tracking drift. In order to make full use of the feature  
293 information of target and reduce the influence of scale variation, we also incorporate a multi-feature  
294 fusion scheme and a scale estimation model in the backbone of the algorithm, which provides a good  
295 basis for later obscuration judgments and model updates.

296 The experimental results show that the Aojmus precedes the other typical tracking algorithms in  
297 terms of tracking precision, which has been increased by 0.6% and 3.8% respectively compared with the  
298 excellent algorithms, MSCF and Staple. Despite the Aojmus is not the best in terms of success rate, it  
299 surpasses the other four compared algorithms with respect to target occlusion, scale variation, fast motion,  
300 out-of-plane rotation and deformation. As the Aojmus is based on the kernel correlation filtering method,  
301 it runs well in real-time with high tracking speed of 74.85 frames per second, striking a good balance  
302 between tracking effectiveness and speed. It can be concluded that the kernel correlation filter-based  
303 multi-indicator occlusion judgement mechanism and adaptive model updating strategy can solve the  
304 common problems of target tracking while maintaining the overall performance. In future, we plan to  
305 investigate the feasibility of synthesizing our method with convolutional neural networks to improve the  
306 overall performance further and extend the application to indoor mobile robot and vehicle violation.

## 307 ADDITIONAL INFORMATION AND DECLARATIONS

### 308 Funding

309 This work is partially supported by the Natural Science Foundation of Fujian Province under the  
310 Grant[2018J01637], the Start-up Research Project under the Grant[GY-Z21064] of Fujian University of  
311 Technology, the New Engineering Research Project (Construction of Electronic and Electrical Practice  
312 Education System and Practice Platform Oriented to New Engineering) of Fujian University of Technology  
313 and the Research Project of Experimental Teaching Reform of Fujian University of Technology under the  
314 Grant [SJ2018002].

### 315 Competing Interests

316 The authors declare there are no competing interests.

### 317 Author Contributions

- 318 • Zhiming Cai designed the mathematical method of tracking algorithm, built the overall framework  
319 of the project, conceived and designed the experiments, authored and reviewed drafts of the paper,  
320 and approved the final draft.
- 321 • Zhuangzhuang Wang completed the whole part of the project, tested the feasibility of the algorithm,  
322 conceived and designed the experiments, prepared figures and tables, authored drafts of the paper,  
323 and approved the final draft.
- 324 • Jianchao Huang and Shujing Chen performed the experiments and processed the data, prepared the  
325 pictures and tables, and analyzed the results.
- 326 • Huabin He performed the experiments, analyzed the data, authored and reviewed drafts of the paper,  
327 and approved the final draft.

### 328 Data Availability

329 The following information was supplied regarding data availability:

330 The public test dataset, OTB-2015 (namely TB-100), used in this article are available on Visual Tracker  
331 Benchmark, at [http://cvlab.hanyang.ac.kr/tracker\\_benchmark/datasets.html](http://cvlab.hanyang.ac.kr/tracker_benchmark/datasets.html).

332 The experiment results underlying this article and the source codes are available at GitHub <https://github.com/fzxincai/Aojmus> Zenodo. <https://doi.org/10.5281/zenodo.7563961>

### 334 REFERENCES

- 335 Al-Battal, A. F., Gong, Y., Xu, L., Morton, T., Du, C., Bu, Y., Lerman, I. R., Madhavan, R., and Nguyen,  
336 T. Q. (2021). A cnn segmentation-based approach to object detection and tracking in ultrasound scans  
337 with application to the vagus nerve detection. In *2021 43rd Annual International Conference of the*  
338 *IEEE Engineering in Medicine Biology Society (EMBC)*, pages 3322–3327, Mexico. IEEE.
- 339 Bertinetto, L., Valmadre, J., Golodetz, S., Miksik, O., and Torr, P. (2016). Staple: Complementary learners  
340 for real-time tracking. In *2016 IEEE Conference on Computer Vision and Pattern Recognition (CVPR)*,  
341 pages 1404–1409, Las Vegas, NV, USA. IEEE.
- 342 Bolme, D. S., Beveridge, J. R., Draper, B. A., and Lui, Y. M. (2010). Visual object tracking using adaptive  
343 correlation filters. In *The Twenty-Third IEEE Conference on Computer Vision and Pattern Recognition,*  
344 *CVPR 2010*, pages 2544–2550, San Francisco, CA, USA. IEEE.
- 345 Cao, Z., Fu, C., Ye, J., Li, B., and Li, Y. (2021). Hift: Hierarchical feature transformer for aerial tracking. In  
346 *2021 IEEE/CVF International Conference on Computer Vision (ICCV)*, pages 15437–15446, Montreal,  
347 QC, Canada. IEEE.
- 348 Dai, K., Wang, D., Lu, H., Sun, C., and Li, J. (2019). Visual tracking via adaptive spatially-regularized  
349 correlation filters. In *2019 IEEE/CVF Conference on Computer Vision and Pattern Recognition (CVPR)*,  
350 pages 4665–4674, Long Beach, CA, USA. IEEE.
- 351 Danelljan, M., Bhat, G., Khan, F. S., and Felsberg, M. (2017a). Eco: Efficient convolution operators  
352 for tracking. In *2017 IEEE Conference on Computer Vision and Pattern Recognition (CVPR)*, pages  
353 6931–6939, Honolulu, HI, USA. IEEE.
- 354 Danelljan, M., Häger, G., Khan, F. S., and Felsberg, M. (2014a). Accurate scale estimation for robust  
355 visual tracking. In *British Machine Vision Conference*, Nottingham, United kingdom. British Machine  
356 Vision Association, BMVA.
- 357 Danelljan, M., Häger, G., Khan, F. S., and Felsberg, M. (2017b). Discriminative scale space tracking.  
358 *IEEE Transactions on Pattern Analysis and Machine Intelligence*, 39(8):1561–1575.
- 359 Danelljan, M., Khan, F. S., Felsberg, M., and Van De Weijer, J. (2014b). Adaptive color attributes for  
360 real-time visual tracking. In *2014 IEEE Conference on Computer Vision and Pattern Recognition*,  
361 pages 1090–1097, Columbus, OH, USA. IEEE.
- 362 Guo, D., Wang, J., Cui, Y., Wang, Z., and Chen, S. (2020). Siamcar: Siamese fully convolutional  
363 classification and regression for visual tracking. In *2020 IEEE/CVF Conference on Computer Vision*  
364 *and Pattern Recognition (CVPR)*, pages 6268–6276, Seattle, WA, USA. IEEE.
- 365 Henriques, J. F., Caseiro, R., Martins, P., and Batista, J. (2015). High-speed tracking with kernelized  
366 correlation filters. *IEEE Transactions on Pattern Analysis and Machine Intelligence*, 37(3):583–596.

- 367 Henriques, J. F., Rui, C., Martins, P., and Batista, J. (2012). Exploiting the circulant structure of tracking-  
368 by-detection with kernels. In *Proceedings of the 12th European conference on Computer Vision -*  
369 *Volume Part IV*, pages 702–715, Florence, Italy. Springer Verlag.
- 370 Huang, Z., Fu, C., Li, Y., Lin, F., and Lu, P. (2019). Learning aberrance repressed correlation filters  
371 for real-time uav tracking. In *2019 IEEE/CVF International Conference on Computer Vision (ICCV)*,  
372 pages 2891–2900, Seoul, Korea (South). IEEE.
- 373 Li, H., Li, Y., and Porikli, F. (2016). Deeptack: Learning discriminative feature representations online  
374 for robust visual tracking. *IEEE Transactions on Image Processing*, 25(4):1834–1848.
- 375 Liu, C., Yao, X., Zhu, Z., Peng, S., and Zheng, W. (2017). A robust tracking method based on the  
376 correlation filter and correcting strategy. In *2017 2nd International Conference on Image, Vision and*  
377 *Computing (ICIVC)*, pages 698–702, Chengdu. IEEE.
- 378 Lu, M. and Xu, Y. (2019). A survey of object tracking algorithms. *Acta Automatica Sinica*, 45(7):1244–  
379 1260.
- 380 Lukežić, A., Vojír, T., Zajc, L. C., Matas, J., and Kristan, M. (2017). Discriminative correlation filter with  
381 channel and spatial reliability. In *2017 IEEE Conference on Computer Vision and Pattern Recognition*  
382 *(CVPR)*, pages 4847–4856, Honolulu, HI, USA. IEEE.
- 383 Ma, C., Huang, J.-B., Yang, X., and Yang, M.-H. (2015). Hierarchical convolutional features for visual  
384 tracking. In *2015 IEEE International Conference on Computer Vision (ICCV)*, pages 3074–3082,  
385 Santiago, Chile. IEEE.
- 386 Meng, L. and Li, C.-X. (2019). Brief review of object tracking algorithms in recent years: correlated  
387 filtering and deep learning. *Journal Of Image And Graphics*, 24(7):1011–1016.
- 388 Nam, H. and Han, B. (2016). Learning multi-domain convolutional neural networks for visual tracking.  
389 In *2016 IEEE Conference on Computer Vision and Pattern Recognition (CVPR)*, pages 4293–4302,  
390 Las Vegas, NV, USA. IEEE.
- 391 Sun, Y., Sun, C., Wang, D., He, Y., and Lu, H. (2019). Roi pooled correlation filters for visual tracking. In  
392 *2019 IEEE/CVF Conference on Computer Vision and Pattern Recognition (CVPR)*, pages 5776–5784,  
393 Long Beach, CA, USA. IEEE.
- 394 Uzcent, B., Hoffman, M. J., Vodacek, A., and Chen, B. (2015). Feature matching with an adaptive optical  
395 sensor in a ground target tracking system. *IEEE Sensors Journal*, 15(1):510–519.
- 396 Wang, M., Liu, Y., and Huang, Z. (2017). Large margin object tracking with circulant feature maps.  
397 In *2017 IEEE Conference on Computer Vision and Pattern Recognition (CVPR)*, pages 4800–4808,  
398 Honolulu, HI, USA. IEEE.
- 399 Wang, N., Xi, M., Zhou, W.-G., Li, L., and Li, H.-Q. (2021). Recent advance in deep visual object  
400 tracking. *Journal of University of Science and Technology of China*, 51(4):335–344.
- 401 Wang, Z., Huang, J., Chen, S., Zhang, Z., and Cai, Z. (2022). Target tracking algorithm based on multi-  
402 feature adaptive fusion in complex scenes. In *Proceedings of the 2022 2nd International Conference on*  
403 *Control and Intelligent Robotics*, page 310–315, Nanjing, China. Association for Computing Machinery.
- 404 Wei, Z. and Kang, B. (2017). Recent advances in correlation filter-based object tracking: a review. *Journal*  
405 *of Image and Graphics*, 22(8):1017–1033.
- 406 Wu, Y., Lim, J., and Yang, M.-H. (2013). Online object tracking: A benchmark. In *2013 IEEE Conference*  
407 *on Computer Vision and Pattern Recognition*, pages 2411–2418, Portland, OR, USA. IEEE.
- 408 Wu, Y., Lim, J., and Yang, M. H. (2015). Object tracking benchmark. *IEEE Transactions on Pattern*  
409 *Analysis and Machine Intelligence*, 37(9):1834–1848.
- 410 Xiao, J., Zhu, S. P., Huang, H., and Xie, Y. N. (2016). Object detecting and tracking algorithm based on  
411 optical flow. *Journal of Northeastern University(Natural Science)*, 37(6):770–774.
- 412 Xie, W.-X. and Zhao, T. (2021). Multi-feature adaptive fusion based target tracking algorithm. *Journal of*  
413 *Signal Processing*, 37(4):603–615.
- 414 Yang, L. and Zhu, J. (2014). A scale adaptive kernel correlation filter tracker with feature integration.  
415 In *13th European Conference on Computer Vision, ECCV 2014*, pages 254–265, Zurich, Switzerland.  
416 Springer Verlag.
- 417 Zeng, Y., Fu, X., Gao, L., Zhu, J., Li, H., and Li, Y. (2020). Robust multivehicle tracking with wasserstein  
418 association metric in surveillance videos. *IEEE Access*, 8:47863–47876.
- 419 Zhang, Z. and Peng, H. (2019). Deeper and wider siamese networks for real-time visual tracking. In *2019*  
420 *IEEE/CVF Conference on Computer Vision and Pattern Recognition (CVPR)*, pages 4586–4595, Long  
421 Beach, CA, USA. IEEE.

- 422 Zheng, G., Fu, C., Ye, J., Lin, F., and Ding, F. (2021). Mutation sensitive correlation filter for real-time  
423 uav tracking with adaptive hybrid label. In *2021 IEEE International Conference on Robotics and*  
424 *Automation (ICRA)*, pages 503–509, Xi'an, China. IEEE.
- 425 Zhou, T. and Liu, Y. (2021). Long-term person tracking for unmanned aerial vehicle based on human-  
426 machine collaboration. *IEEE Access*, 9:161181–161193.